A synthetic lethal interaction with a viral-induced hypomorph of GBF1

Arti Navare[1], Fred D Mast[1], Jean Paul Olivier[1], Thierry Bertomeu[2], Maxwell Neal[1], Jasmin Coulombe-Huntington[2], Mike Tyers[2] and John D Aitchison[1,3,4]

1. Center for Global Infectious Disease Research, Seattle Children's Research Institute, Seattle, Washington, USA
2. Institute for Research in Immunology and Cancer, Université de Montréal, Montreal, Quebec, Canada
3. Department of Pediatrics, University of Washington, Seattle, Washington, USA
4. Department of Biochemistry, University of Washington, Seattle, Washington, USA

Corresponding author:
John D Aitchison, PhD
Center for Global Infectious Disease Research
Seattle Children's Research Institute
307 Westlake Avenue North, Suite 500
Seattle Washington, 98109-5219
Tel: (206) 884-3XXX
Fax: (206) 884-3XXX
john.aitchison@seattlechildrens.org

Keywords:
synthetic lethality, viral-induced hypomorph, GBF1, genetic interactions, poliovirus

Abstract
Viruses co-opt host proteins to carry out replication of the virus. Host proteins thus repurposed may become functionally compromised, a situation analogous to a loss-of-function allele, which we term a viral-induced hypomorph. Tumor-specific loss-of-function alleles have successfully been targeted with drugs perturbing proteins encoded by the synthetic lethal partners of these cancer-specific mutations. Synthetic lethal interactions with viral-induced hypomorphs have yet to be demonstrated, an important first step in the development of antiviral therapeutic strategies based on the principle of synthetic lethality. We focused on Golgi-specific brefeldin A-resistance guanine nucleotide exchange factor 1 (GBF1), a proviral host factor for many RNA viruses. A chemogenomic screen using the GBF1-specific inhibitor, golgicide A, identified 57 putative synthetic lethal partners of GBF1, including ADP-ribosylation factor 1 (ARF1). Using a poliovirus protein, 3A, to induce a GBF1-hypomorph, we observed synthetic lethality in the context of a shRNA-mediated knockdown of ARF1. These results provide a proof-of-concept that virus-induced hypomorphs are sensitive to perturbation by synthetic lethal interaction and open up a new avenue for antiviral therapeutic development.

Introduction

RNA viruses are prevalent and pervasive pathogens and cause many global health crises [1]. They typically have high mutation rates enabling them to rapidly adapt to new cell types, infect new host species, evade host immune responses, and quickly develop antiviral drug resistance[2]. Currently, the repertoire of FDA approved antivirals is limited, targeting only eight out of the known 214 human-infecting RNA viruses[3]. Almost exclusively, these FDA approved drugs are all designed to target viral proteins[3,4]. This dearth of antivirals is likely impacted by the many challenges faced in antiviral drug development, including the small list of target viral proteins due to their compact genomes, the quick emergence of escape mutants due to the high mutation rates prevalent in many RNA viruses, and the limited therapeutic range of antivirals due to the diversity of RNA virus serotypes which, akin to antimicrobial resistance, has led to limited strain-specific use, or even discontinuation of use, for many antivirals[3,5–7]. Yet, the same compact-sized genome that gives these viruses an edge over antivirals also makes them obligatory pathogens that rely on host proteins for survival. The idea of exploiting this over-reliance on their host to develop host-directed antivirals is gaining traction[8].

Host-based therapies expand opportunities for treating viral infections[9–11]. To proliferate, viruses must co-opt common host pathways and cellular machineries by forming protein-protein interactions with host proteins[12–17]. Due to the essential requirement of these interactions, they are likely to be conserved within viral lineages and can be targeted for developing broad-spectrum therapeutics[18–20]. Recently, an analysis of published virus-host interaction datasets revealed RNA viruses frequently engage so-called “multifunctional host proteins”, a set of 282 highly connected proteins as assessed by their protein-protein interaction networks[3,21]. Targeting these multifunctional host proteins, many of which have FDA approved drug inhibitors, could, disrupt several crucial steps of viral replication. Inhibiting a virus by targeting the host reduces the possibility of drug resistance and is potentially broad-spectrum if more than one virus relies on the same host protein. However, inhibiting viruses by targeting these host proteins with drugs may also elicit adverse effects on the host due to the loss of function of the targeted host proteins. Thus, the advantages and disadvantages must be balanced with considering host-based therapy. Therefore, alternative approaches that target the virus through the host, but that don’t have serious adverse side effects are required.

The principle of synthetic lethality offers an opportunity for selectively targeting virus infected cells by drugging synthetic lethal interactors of virus-targeted multifunctional protein hubs[8]. Synthetic lethality occurs between two genes occurs when a loss-of-function mutation in either gene has little impact on cell viability, but becomes detrimental when paired with together and results in cell death[22] (Fig 1A). Such lethal genetic combinations, known as “synthetic lethal pairs”[23], are one of many forms of genetic interactions that can occur within cells[24–26]. The existence of synthetic lethality reveals important aspects of the genetic architecture of cells, demonstrating the presence of genetic buffering in organisms due to functional redundancy[26,27]. This synthetic lethal concept has been successfully applied to cancer therapy and host-targeted drug development[28–32](Fig 1B). For example, loss-of-function mutations in the DNA repair genes encoded by breast cancer type 1 and 2, *BRCA1* and *BRCA2,* cause breast and ovarian cancer but exhibit enhanced sensitivity to inhibitors of poly ADP-ribose polymerase (*PARP*), another DNA repair enzyme[30]. PARP inhibitors selectively killed cancerous cells carrying the loss-of-function *BRCA* mutation while sparing noncancerous cells[33] and in a clinical trial PARP anticancer drugs showed a significantly longer progression-free period in patients with breast cancer[34]. Synthetic lethality driven anticancer therapy provides avenues for improved drug specificity and efficacy at lower doses, thereby limiting side effects. Here, we extend the application of this synthetic lethality principle to host-derived antiviral targets.

Virus infection can be thought of as a perturbation of the host PPI network. Interactions between virus and host proteins usurp normal protein functions and rewire host PPIs. Consequently, infected cells exhibit altered metabolic requirements[35], signaling pathways[36], and

intracellular transport pathways[37] relative to the noninfected cells. In such situations the infected cells become dependent upon the other protein partner of the virus-interacting host factor that perform redundant or overlapping function. Rationale targeting of synthetic lethal protein pairs in which the function of one partner is reduced specifically in the infected cell; a situation equivalent to the non-functional gene in cancer, is a novel framework for taking advantage of the intrinsic differences of infected cells to achieve selective targeting (Fig 1C). We hypothesize that viral-host PPIs generate protein-based, viral-induced (*vi*)- *hypomorphs* of host factors in infected cells, thereby specifically sensitizing infected cells to targeting synthetic lethal/synthetic sick partners of these *vi-hypomorphs*. To test our hypothesis, we selected the Golgi-specific brefeldin A-resistance guanine nucleotide exchange factor GBF1[38]. *G*BF1 mediates recruitment of coat proteins, lipid modifying enzymes, and protein tethers to Golgi membranes. It thus plays a central role in vesicular transport through the Golgi, the structural integrity of Golgi membranes, and the maintenance of lipid homeostasis[39–43]. With its dynamic membrane-modulating functions GBF1 has also been implicated in coatomer-dependent protein delivery to lipid droplets[43,44]

GBF1 has emerged as a critical host factor in the replication of *Picornaviridae, Coronaviridae, Flaviviridae*, *Herpesviridae*, *Filoviridae*, and *Rioviridae* families of RNA viruses[15,45–51]. Many RNA viruses encode for proteins that bind GBF1 directly, including the nonstructural proteins 3A of poliovirus[52,53] and coxsackievirus[54,55], and nonstructural protein 5 of dengue[15]. Poliovirus 3A redistributes GBF1 to viral replication complexes during early stages of replication and subverts its guanine nucleotide exchange factor (GEF) function in the infected cells[15,55–58]. GBF1 is thus a suitable candidate for designing broad-spectrum antivirals based on synthetic lethality because (i) GBF1 is directly targeted by nonstructural viral proteins , (ii) these interactions attenuate GBF1 functions and create a *Vi-induced hypomorph* of GBF1, and, (iii) GBF1 has a specific small molecule inhibitor, Golgicide A (GCA)[40]. To validate this concept, we performed a genome-wide chemogenomic CRISPR screen to identify synthetic lethal gene partners of GBF1 using GCA. We then silenced the putative synthetic lethal gene of GBF1 and used a viability assay to validate the top candidates from GCA CRISPR screens. Finally, we employed shRNA-mediated silencing of a validated synthetic lethal gene, ARF1, and compared cell viability of ARF1- knockdown cells when GBF1 is attenuated during ectopic expression of poliovirus protein 3A.

Results and Discussion:

In order to identify putative synthetic lethal partners of GBF1, we screened a high-complexity extended-knockout CRISPR library of 278K single guide RNAs (sgRNAs) that target 19,084 RefSeq genes in NALM-6 human pre-B leukemia cells[59]. These cells harbor a genomic and doxycycline-inducible Cas9 that enables regulatable, uniform and robust gene silencing across the pooled library[60]. Relative changes in sgRNA frequencies were obtained from sequencing populations of the CRISPR libraries cultured in the presence or absence of GCA, a potent inhibitor of the GTPase activity of GBF1[40]. The concentration of 4 μM GCA, was determined prior to the screen to maximize both enrichment (i.e., positive selection for rescue of compound toxicity) and depletion (i.e., negative selection for synthetic lethal interactions)sgRNA frequencies were determined by sequencing and relative fold changes in sgRNA abundances between GCA treated and untreated samples were reported (Fig 2A).

Relative gene frequencies following GCA treatment were scored using two different methods. The first ranks sgRNA frequencies based on the average $\log_2$ fold-change in sgRNA abundance between the treated and control samples. The second provides a statistical score incorporating the average natural log single-tailed p-value of the individual sgRNAs for each

gene with >=20 reads, termed RANKS (Robust Analytics and Normalization for Knockout Screens)[59]. The sgRNA p-value is estimated from its relative log_2-read-frequency-fold-change as compared to the fold-change distribution of non-targeting control sgRNAs. Genes with a statistically significant depletion of individual sgRNAs have a RANKS score below zero, and those with sgRNA enrichment relative to the untreated samples have a RANKS score above zero Generic effects were accounted for by taking into consideration prior establishment of gene essentiality in published CRISPR screens[59].

Using a FDR of <0.05, there were 57 underrepresented genes and 45 overrepresented genes in the GCA treated samples relative to control (Fig 2A: white circles). The underrepresented genes are putative synthetic lethal partners of GBF1. We searched this list against the drug gene interaction database for potential 'druggability' (http://dgidb.org/search_categories) and selected five druggable, putative synthetic lethal interactors of GBF1 (Fig 2A,B). ADP-ribosylation factor 1 (*ARF1*) is a small GTPase that regulates the recruitment and assembly of COP I on Golgi and ERGIC membranes[61]. Heat-shock protein 90 (HSP90) is a protein chaperone with ATPase activity[62]. C-terminal Src kinase (*CSK*) negatively regulates Src family kinases with roles in cell growth, differentiation, migration and immune response[63]. Protein kinase, AMP-activated, alpha 1 (PRKAA1) is the catalytic subunit of the 5'-prime-AMP-activated protein kinase (AMPK) with roles in regulating cell stress and metabolism[64]. Casein Kinase 2 Alpha 1 (CSKNK2A1) is involved in various cellular processes, including cell cycle control, apoptosis, and circadian rhythm[6566]. These five putative synthetic gene partners of GBF1 were silenced in Hela cells along with methylsterol monooxygenase 1 (*MSMO1*), included as a control because it showed insignificant depletion or enrichment in sgRNA abundance, and *ARF4*, which exhibited suppressive effects in our CRISPR screen and was the topmost significantly over-represented gene upon GCA treatment (Fig 2A). The KD cell lines were incubated with 1.5 μM or 4 μM of GCA/DMSO-alone for 48 h before measuring viabilities. Synthetic lethal effects of combining GCA with shRNA knockdown were observed in *ARF1*KD cells with only 40% or 50% viability as compared to the DMSO-treated cells at 4 μM and 1.5 μM GCA concentration respectively (Fig 2B). When the viability of each KD cell line was compared to that of the *MSMO1*KD control, the decrease in the viability was statistically significant for *ARF1*KD at both concentrations, confirming the results of the chemogenomic screen (Fig 2A).

Next, we asked if functional attenuation of GBF1 could be achieved with ectopic expression of poliovirus protein 3A, which recruits GBF1 to sites of poliovirus replication [ref]. Poliovirus isolates expressing a modified FLAG tagged 3A have previously been reported to be stable and yield 3A-tagged viruses with similar fitness to the wild-type untagged virus[53]. The modified FLAG tag (FLAG*) is similar to the conventional 8-amino acid (DYKDDDDK) FLAG tag , but with the last aspartic acid replaced by tyrosine and is recognized by anti-FLAG antibodies[53] (Fig 3A). N-terminal, FLAG*-tagged 3A, or an empty plasmid control was transiently transfected into Hela cells for 24 h. FLAG*-3A and associated proteins were affinity purified on magnetic beads conjugated with anti-FLAG antibodies. Isolated complexes were washed, and the eluate along with a fraction of the load and wash volumes were resolved by SDS-PAGE, transferred to nitrocellulose, and probed with anti-FLAG and anti-GBF1 antibodies (Fig 3A). A band of ~ 10 kDa was detected in the eluate corresponding to the FLAG*-3A protein. A high molecular weight band of ~ 200 kDa, corresponding to GBF1, was detected in eluate of the FLAG*-3A transfected cell immunoprecipitation, but not in the eluate of the immunoprecipitation of the empty plasmid control (Fig 3A). This observation confirmed that the ectopically expressed FLAG*-3A protein retained its ability to physically interact with GBF1, as reported previously[53].

We next tested if the physical interaction between 3A and GBF1 had consequences for GBF1 function, i.e. whether 3A is able to induce a hypomorph of GBF1. Hela cells were transduced with lentivirus delivering an empty control or FLAG*-3A and cells were fixed and

immunostained with anti-FLAG-647 (red) and anti-GBF1-488 (green), antibodies (Fig 3B). GBF1 was visualized as puncta enriched in a juxtanuclear position consistent with a Golgi localization in the control cells (marked by red arrows). This juxtanuclear enrichment was lost in 3A transduced cells and the GBF1 puncta were instead found redistributed throughout the cytoplasm (Fig 3B). We quantified this redistribution by measuring the distance of all GBF1 puncta from the nearest nucleus for each cell in the dataset (Fig 3C,D). This quantification revealed an increase in GBF1 puncta localized away from the nucleus in 3A transduced cells that was statistically significant compared to control (Fig 3C,D). The depletion of Golgi-localized GBF1 upon expression and interaction with poliovirus 3A is consistent with 3A inducing a GBF1-hypomorph.

Having identified ARF1 as a synthetic lethal interactor of GBF1, and established that a GBF1 hypomorph could be induced by expression of poliovirus 3A, we next asked if the 3A-induced hypomorphic state of GBF1 was sufficient to drive a synthetic lethal interaction in cells depleted of ARF1. Hela cells were treated with shRNA to ARF1, or MSMO1 as a control, with knockdown of protein expression verified by western blot (Sup Fig 1). FLAG*-3A or an empty plasmid control was transiently transfected into both knockdown cell lines and expression of FLAG*-3A was detected by flow cytometry analysis (Fig 4A). The viability of ARF1 knockdown cells was significantly decreased by the expression of FLAG*-3A (Fig 4B). By comparison, the MSMO1 knockdown cells were not significantly affected.

Synthetic lethality is conventionally described as a type of genetic interaction between two nonessential genes that participate in a parallel redundant pathway to carry out essential function, where mutations in either one alone does not affect cell viability, but mutations in both genes results in cell death[67]. In this manuscript, we have extended the idea of synthetic lethality to interactions involving a virus-induced hypomorph. In poliovirus, the viral replication complex protein 3A physically interacts with GBF1[52,53] (Fig 3A) and re-localizes it to the replication complexes[58] [ref]. We show here, that this relocalization sensitizes and reduces the viability of cells depleted of ARF1 (Fig 4B).

In summary, viral-host protein-protein interactions that result in the functional attenuation of the host factor offer a promising avenue for therapeutics based on the principle of synthetic lethality. In this context, the infected cell becomes selectively dependent upon the otherwise nonessential synthetic lethal partner of the virus-induced hypomorph. Our proof-of-concept experiments provide a rational approach for rapidly identifying these novel antivirals.

Materials and Methods

Cell culture and plasmids

HeLa cells were maintained in High glucose DMEM media containing 10% fetal bovine serum, and supplement with 20 mM L-glutamine, 1× nonessential minimal media, 1× Sodium Pyruvate and 10 mM HEPES buffer (complete media).

Agarose stabs of *E. coli* (DH10B) with mammalian expression vector pD2109-EF1 was purchase from ATUM (Newark, CA USA). pD2109-EF1 encodes Poliovirus protein 3A with a modified FLAG tag (DYKDDDYK) inserted at the N-terminus. The modified FLAG tag (referred here as FLAG*), contains a Tyrosine (Y) residue at position 7 instead of aspartic acid residue (D) found in a typical FLAG tag sequence. A complete sequence of the FLAG*-3A protein with the inserted FLAG* tag (in bold) is as follows:
GPLQYK**DYKDDDYK**DLKIDIKTSPPPECINDLLQAVDSQEVRDYCEKKGWIVNITSQVQTERN INRAMTILQAVTTFAAVAGVVYVMYKLFAGHQ
Plasmid DNA was purified from the agarose stabs using NucleoBond Xtra Midiprep kit by following the manufacture's protocol. FLAG*-3A protein was expressed in HeLa cells by plasmid DNA transfection or transduced by lentivirus (spinfection). We used an empty plasmid pLKO1.puro with comparable size to pD2109-EF1 as a control for transfections.

GCA CRISPR screening

Genome-wide custom extended-knockout (EKO) pooled library was created in a B-cell lymphoma line using a published protocol[59]. Briefly, a clone of the NALM-6 cells expressing Cas9 under a Tet-ON promoter was transduced with the 278K sgRNAs followed by selection over blasticidin, and induction of knockdown of genes with 2 µg/mL doxycycline over a 7 day period. At that time (day 0), the EKO library was split into two flasks, one containing 4 µM GCA and the other containing media alone and each library flask was grown for 8 more days. During this period, cell counts were made every two days and population doublings occurred during the 8 day time were estimated. sgRNA sequences were recovered by PCR of genomic DNA, reamplified with Illumina adapters, and sequenced on an Illumina HiSeq 2000 instrument.

RANKS scores and determination of sgRNA frequencies in GCA-treated samples was performed as described[59].

Lentivirus stock preparation

Glycerol stocks of the validated MISSION shRNA vectors for ARF1, PRKAA1, HSP90, CSK, CSNK2A, MSMO1 and ARF4, were obtained from Sigma 32 Aldrich (St. Louis, MO). 10x stocks of non-replicating lentiviral stocks were generated by transfection of HEK293-FT cells as follows: 4×10^6 HEK293-FT cells were plated on poly-L-lysine coated 10 cm dishes to achieve 70-80% confluency at time of transfection. Next day, transfection mixtures were prepared by mixing 20 µL Polyethyleneimine MAX (Polysciences Inc, Warrington, PA) prepared at 1 mg/ml, together with 4.75 µg of transgene shRNA constructs, 1.5 µg of viral envelope plasmid (pCMV-VSV-G), and 3.75 µg of viral packaging plasmid (psPax2). After incubating for 10 min at room temperature in DMEM, transfection complexes were added dropwise to cells. After overnight incubation, cells were washed to remove transfection mixtures and replaced with 10 mL of pre-warmed media. Lentivirus-containing supernatant was harvested 48 hours later, centrifuged for 5 minutes at 4,000 rpm to remove cell debris, passed through 0.45 µm syringe filters, and ultracentrifuged for 4 hours at 24,000 rpm. Supernatants were decanted and pelleted lentiviruses were re-suspended in 0.1

mL Opti-MEM to obtain 10x lentivirus concentrates and stored at -80 ˚C until use. Similar protocol was used to prepare 10x lentivirus stocks of FLAG*-3A.

shRNA-mediated gene Knockdowns

To induce knockdown of the top putative GBF1 SL genes, 300,000 HeLa cells were transduced with lentiviral supernatants in 6-well plates. At time of plating, 10 x lentivirus concentrates were diluted in1 mL of Opti-MEM containing $8x10^{-3}$ µg/mL of polybrene (Sigma Aldrich 45 St. Louis, MO) and incubated overnight in the cell culture incubator. Next day, transfection mix was replaced with 2 mL of pre-warmed complete media and incubated for 24 hours. In order to select for cells with stable integration of shRNA transgenes, overnight media was replaced with complete media containing 1.5 µg/mL puromycin. Cells were selected for at least 3 days prior to experiments. At the time of the experiments, the stably silenced knockdown cell lines (ARF1KD, HSP90KD, CSKKD, CSNK2AKD, PRKAA1KD, MSMO1KD, and ARF4KD) were harvested by trypsinization in 0.25% trypsin-EDTA, washed in pre-warmed PBS, cells were counted, and a small aliquot was cells were saved for western blot analysis to verify protein level knockdown efficiencies for each gene.

Western Blot analysis

Cell pellets of the KD cell lines were re-suspended in a chilled IP lysis buffer (20 mM HEPES, 1% Triton X-100, 0.5% Sodium Deoxycholate, 110 mM KoAc, 2 mM $MgCl_2$, 25 mM NaCl, and protease inhibitors (pH = 7.5)) and lysed by sonicating for 1 minute using a probe sonicator operated at an amplitude of 10 with 10 seconds on/ off cycle. Lysates were centrifuged at 50,000 rpm for 5 minutes and supernatants were transferred into a fresh tube. Protein concentrations were determined using BCA assay (ThermoFisher Scientific) and working solutions of lysates at concentrations of 15-30 µg total proteins per 30 µL were prepared with 1X of LDS sample buffer + reducing reagent (NuPAGE, ThermoFisher Scientific) followed by heating at 70 ˚C for 20 minutes on a Thermomix. 30 µL of the reduced lysate was loaded per well on 4-20% or 12% (for ARF1KD and ARF4KD) Bis-Tris gels (NuPAGE, ThermoFisher Scientific) and protein bands were resolved at a constant voltage of 170 V for 1 hour. Protein bands were transferred on PVDF membranes using Xcell2 blot module (ThermoFisher) for 2 hours at 37 V and membranes were blocked in 5% Milk/TBST for an hour at room temperature. After blocking, membranes were incubated with primary antibodies against proteins of interests: ARF1 (ab58578;1:1000), ARF4(ab190000; 1:1000), HSP90 (GTX101448; 1:1000), CSK(GTX107916; 1:500), CSNK2A (13-453;1:500), PRKAA1(ab32047; 1:1000) and MSMO1(ab116650; 1:500) and washed thrice in TBST buffer before incubating with appropriate HRP-conjugated secondary antibodies (Goat anti-mouse or anti-rabbit; 1:2500 dilution). Following incubation, membranes were washed and developed using chemiluminescent substrates (Advansta WesterBright). Images were acquired using FluorChem imager (Protein Simple), and membranes were stripped using a stripping buffer (ThremoFisher), blocked, incubated with HRP-anti-βactin antibody (ab49900; 1:25,000) and imaged as before. Images were processed using Adobe photoshop (for adjusting brightness and contrast) and InDesign (for adding labels) tools.

FLAG*-3A lentivirus spinfection and direct plasmid transfection

<u>Spinfection:</u> Spinfections were carried out for determining lentivirus titers in HeLa cells and also for the proof-of-concept experiment using ARF1KD and MSMO1KD cells where the FLAG*- 3A protein was expressed for the first 48-hours before GCA treatment. For lentivirus titration, 300,000 HeLa cells were spinfected in 6-well plates. For the proof-of-concept experiment, 5000

ARF1KD and MSMO1KD cells were spinfected per well in a 96-well plate. HeLa cells were seeded a day before and next day, 10x lentivirus stock of was thawed and diluted to 1x in pre-warmed Opti-MEM containing $8x10^{-3}$ µg/mL polybrene. Overnight media was removed and 1 mL of 1x lentivirus was added dropwise. Plates were spun for 1 hour at 2,400 rpm using a benchtop centrifuge. After 1hour of spinning, and 2 mL pre-warmed complete media was added on top of each well and cells were stored in the incubator at 37 °C overnight. The next day, lentivirus-containing media was removed and replaced with complete media. The percentage of transduced cells expressing FLAG*-3A expressing cells was determined by flow cytometry analysis.

Transfection: FLAG*-3A plasmid DNA were directly transfected in HeLa cells for performing immunofluorescent imaging (IF) and co-immunoaffinity (Co-IP) purification assays using TransIT transfection reagent (Mirus) by following manufacturer's recommended protocol. Briefly, transfection mix was prepared in a serum free Opti-MEM media by adding FLAG*-3A DNA and TransIT reagent in a ratio of 1: 3 (µL: µL) and mixture was incubated for 30 minutes at room temperature. After incubation, the transfection mix volume equivalent to 1 µg and 15 µg total DNA was added to 60,000 HeLa cells (IF) and $3x10^6$ cells (Co-IP), respectively. After 24 h of transfection, cells were processed as per the IF and Co-IP protocols described below.

Flow cytometry assay

Transduced HeLa cells were trypsinized using 0.05% Trypsin-EDTA and transferred into a U-bottom 96-well plate. Cells were washed twice in PBS/10%FBS and incubated with Live/Dead Fixable stain (Ex/Em: 416/451; ThermoFisher Scientific) for 15 minutes on ice. Excess stain was removed by washing twice and cells were fixed using Fixation/Permeabilization solution (BD Cytofix/cytoperm) for 30 minutes on ice. Fixed cells were washed in Perm/block BD buffer and stained with PE-conjugated anti-FLAG antibody (Biolegends, PE anti-DYKDDDDK Tag Antibody) for 1 hour on ice. After staining, cells were washed thrice in the perm/blocking buffer and analyzed by LSRII flow cytometer (BD Biosciences) and FlowJo software (Tree Star, Inc.).

IF imaging microscopy

HeLa cells were plated in 12 well plates containing at the cell density of 60,000 and transfected with FLAG*-3A and an empty plasmid (control). Cells were fixed with 2% formaldehyde (Sigma) at 24 hour post-transfection, permeabilized with 0.1% Trition X-100, and blocked with PBS/2%BSA/0.1% Triton X-100 (blocking buffer). After blocking, cells were incubated with rabbit anti-GBF1 (abcam, ab86071) and mouse anti-FLAG (Sigma F1804) and mouse anti-ERGIC antibodies for one hour followed by 1 hour staining with goat anti-rabbit alexa flour 488 (for detecting GBF1), and goat anti-mouse alexa fluor 594 (for detecting FLAG*3A) secondary antibodies. Slides were mounted on Nuclei were stained with DAPI (ProLog antifade moutant) and alexa flour 647 conjugated anti-ERGIC antibody (Life 90 technologies) was used for the ER-Golgi intermediate compartment visualization. Images were acquired with a 100× 1.4, Oil objective (Olympus) on a DeltaVision Elite High Resolution Microscope (GE Healthcare Life Sciences). Image z stacks were acquired with 0.2 µm steps and 25 - 27 images per stack. Images were deconvolved with the manufacturer's supplied deconvolution software (SoftWoRx)[68,69].

GBF1 quantitation

Images were further processed using Imaris software (Bitplane) to quantify the number of GBF1 puncta per cell. Fluorescent intensities from all channels were summed into a new channel and

cell surfaces were defined based on summed intensity of this new channel using the Cell Surface command function. Background signal outside the mapped cell surfaces was removed from further processing. Next, cell nuclei volumes were defined using the DAPI channel and cell boundaries defined using the 'one nucleus per cell' function in order to split touching cells. Next, GBF1-488 channel was selected for detecting GBF1 punctate using the 'detect vesicle' function with 'different vesicle sizes' option turned on. After this last step, cell statistics values for 'Vesicle intensity sum' and vesicle distance to closest nucleus' for each GBF1 punctate were exported for all 20 images acquired from control samples, and from 10 images of FLAG*3A transfected cells in which the expression levels of PV 3A were detected above background noise.

Co-IP analysis of PV 3A-GBF1 interaction

HeLa cells were transfected with 1 µg DNA of each of the FLAG*-3A and an an empty control plasmid. At 24 h post-transfection, cells were lysed using mild sonication in 20 mM HEPES IP lysis buffer under, cell debris was removed by centrifugation. Please refer to the 'Western Blot analysis section' for more details on the cell lysis conditions. Total protein concentrations were measured using BCA assay and 100 ug lysate of each sample was used in the immunoprecipitation. We used a published protocol[70] to conjugate 8 µg of anti-FLAG (F3165, Sigma Aldrich) antibody to 10 µg of magnetic beads (M-270 Epoxy Dynabeads, ThermoFisher Scientific). The conjugated beads were washed and re-suspended in the IP lysis buffer and aliquots equivalent to 3 mg beads were added to the clarified lysates. Lysates were rotated overnight in a cold room and washed three times with the IP lysis buffer. Bound proteins were eluted with 50 µl 1× lithium dodecyl sulfate and resolved on 4-20% Bis-Tris NuPAGE gel. Approximately 10% of the eluate was resolved on a 3-8% Tris-Tricine gel to confirm expression and immunoaffinity enrichment of the FLAG*-3A bait. Proteins were transferred to PVDF membranes and immunoblotted with anti-GBF1 antibody (1:1000 dilution GTX102644, GeneTex) and anti-FLAG antibody.

Cell viability assay

Cell viability assays were performed in 96-well plates (black with clear flat bottoms) using the CellTiter-Blue reagent. (Promega). Working concentrations of GCA/ were prepared by diluting a 10 mM stock (in DMSO) in complete media. Equimolar solutions lacking the drug were prepared by diluting neat DMSO. Overnight seeding media was replaced by 100 µL of GCA or DMSO working solutions, and cells were grown for 48 hours. At the end of the experiment, 20 µL of the CellTiter-Blue reagent was added, and the fluorescence was measured 2 hours-post addition of the reagent using a Glomax Multi Detection plate reader (Promega).

For the viability assay validating GBF1-SL candidates, 20,000 cells of each KD cell lines were seeded per well in 200 µL media and treated the drug or DMSO 24 hours later. For the proof-of-concept viability experiments, 5,000 cells of ARF1KD and MSMO1KD were seeded and first transduced with FLAG*-3A lentivirus over 48-hour and then treated with GCA. Cell viability was calculated by dividing fluorescent values of GCA-treated conditions by fluorescent values of DMSO-treated conditions for each KD cell line. For the proof-of-concept viability experiment, fluorescent values of the ARF1KD cells were divided by fluorescent values of MSMO1KD cells at each experimental condition). *P* values were determined in GraphPad Prism 8 by comparing relative viabilities between KD cell lines and MSMO1KD controls at each condition using Welch's ANOVA test.

Figure 1

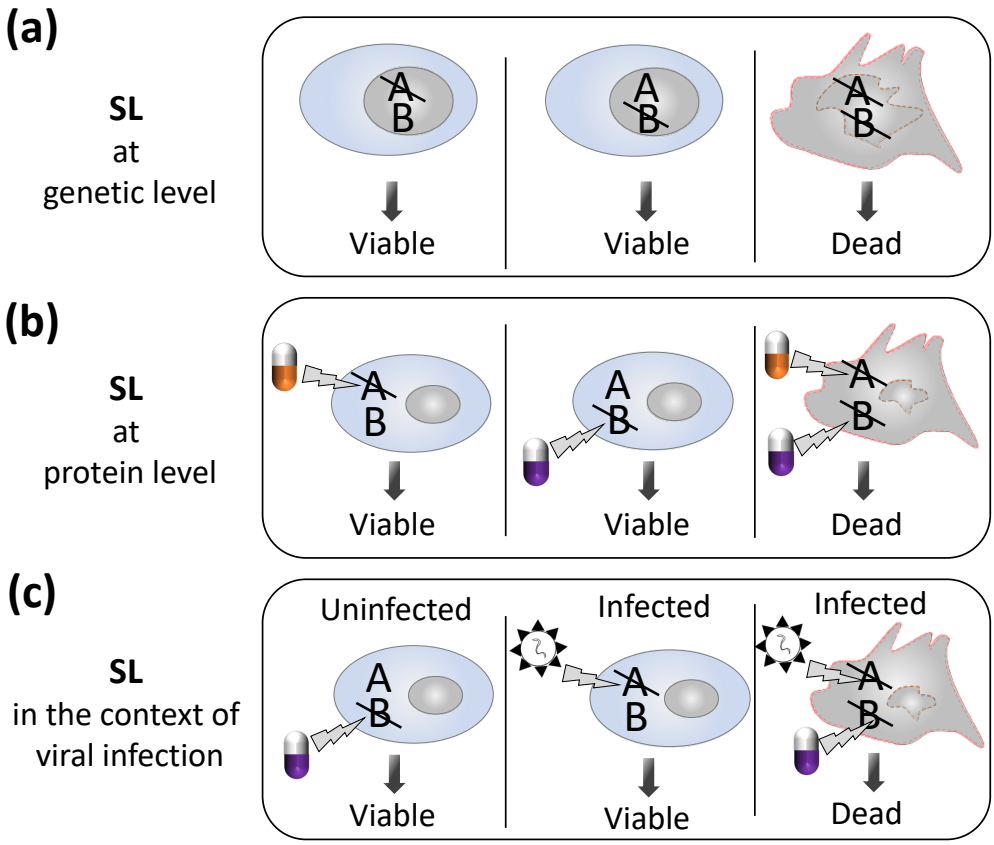

Figure 1: Extending the principle of synthetic lethal interactions to virus-infected cells. (**a**) Synthetic lethality is classically viewed as an extreme genetic interaction occurring between two genes. Here, genes 'A' and 'B' are not essential, and the cell is viable upon the loss of either gene, individually. However, when these deletions are combined in a cell, this double loss of function critically impairs the cell, resulting in its death. Such gene-gene combinations are termed synthetic lethal partners. (**b**) Synthetic lethality can also occur by targeting the protein products of genes 'A' and 'B'. Here, an inhibitory drug of protein A or B does not impact cell viability when delivered individually but become are toxic to the cell when delivered in combination as both synthetic lethal partners have been inhibited. (**c**) Viral infections provide opportunities for synthetic lethality to occur when the function of one of the synthetic lethal partners is attenuated by direct binding to a viral protein. Such a *virus-induced hypomorph* is thus sensitized to the inhibition of its synthetic lethal partner by an inhibitory drug.

Figure 2

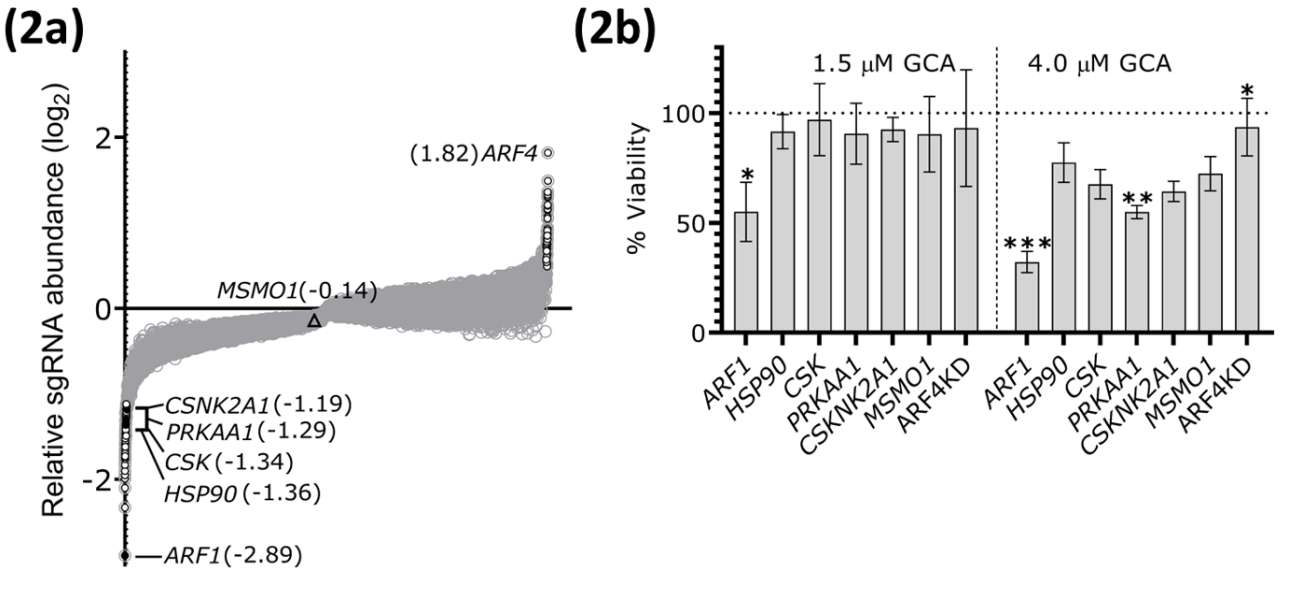

Figure 2: Genome-wide CRISPR GCA screens and confirmation of SL gene partners of GBF1. **A.** CRISPR library of Nalm-6 cells was screened with 4μM GCA to identify synthetic lethal gene partners of GBF1. The $\log_2$ fold change of sgRNA frequencies of all genes from GCA-treated cells were compared to the control (grey circles). Genes passing the 0.05 FDR cut off are shown in white circles. Genes with significantly depleted sgRNA abundances upon GCA treatment represent putative GBF1- SL interactors. **B. Viability assay.** *ARF1*, *HSP90*, *CSK*, *PRKAA1, CSNK2A1*, *MSMO1*, and *ARF4* were silenced in Hela cells via shRNA-mediated lentivirus transductions and treated with 1.5 or 4 μM GCA. Cell viability was measured using CellTiterBlue reagent and the percent viability relative to DMSO-treated cells was determined. The viability of the KD cell lines was compared to *MSMO1*KD using a Brown Forsythe and Welch ANOVA multiple comparison test and statistically significant differences are indicated (* if *p*-value < 0.01; ** if *p*-value < 0.001; *** if *p*-value <0.0001).

Figure 3

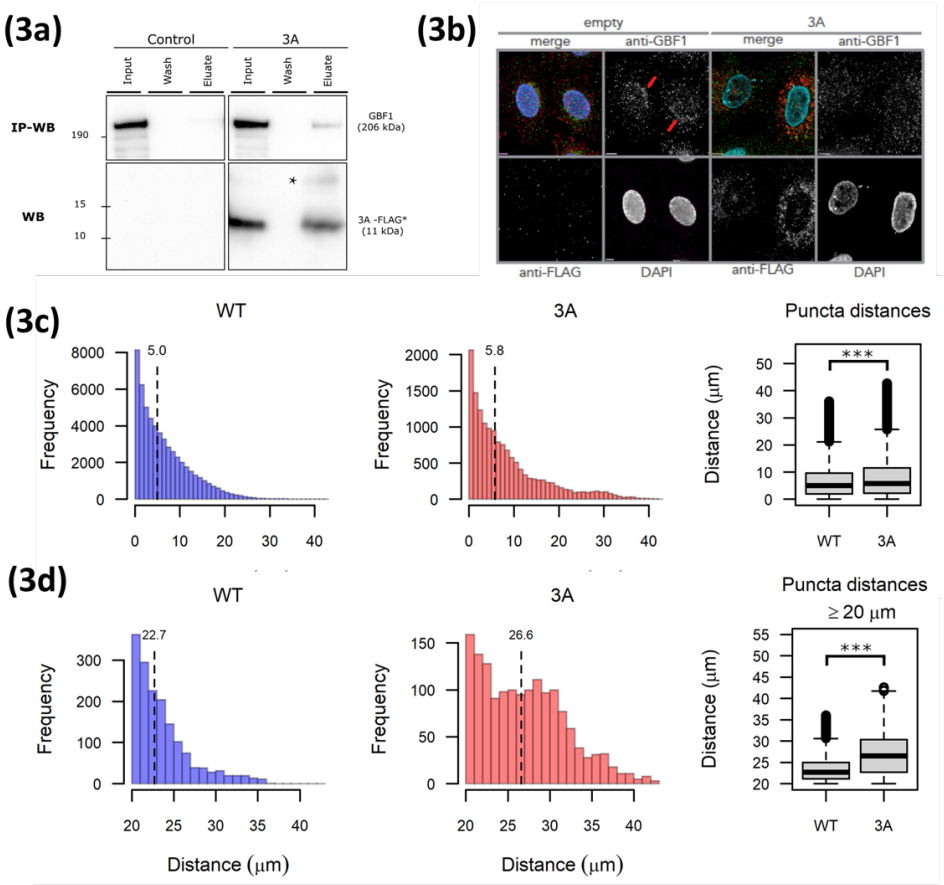

Figure 3: **Poliovirus nonstructural protein 3A induces a *Vi-hypomorph* of GBF1. A.** Hela cells were transfected with FLAG* tagged poliovirus 3A or an empty control plasmid for 24 h. Equal amounts of lysates were immunoaffinity enriched for bound protein complexes to the tagged viral protein. Affinity captured proteins were eluted and resolved on SDS-PAGE along with 1% of the total input lysate and the final wash. Protein were transferred to nitrocellulose membrane and immunoblotted using anti-GBF1 (Top) and anti-FLAG (bottom) antibodies. **B.** Hela cells transfected with FLAG* tagged poliovirus 3A or an empty control plasmid were fixed, and stained with fluorescently labeled antibodies against FLAG and GBF1. **C-D.** Images of GBF1 were analyzed using Imaris software and the distances of each GBF1 puncta to the nearest nucleus was determined and plotted across the entire distance range and between 20 μM to 40 μM for both control and 3A-transfected samples. The corresponding box plots show statistically significant differences in GBF1 distribution between the two samples (*** *p*-value <0.0001).

Figure 4

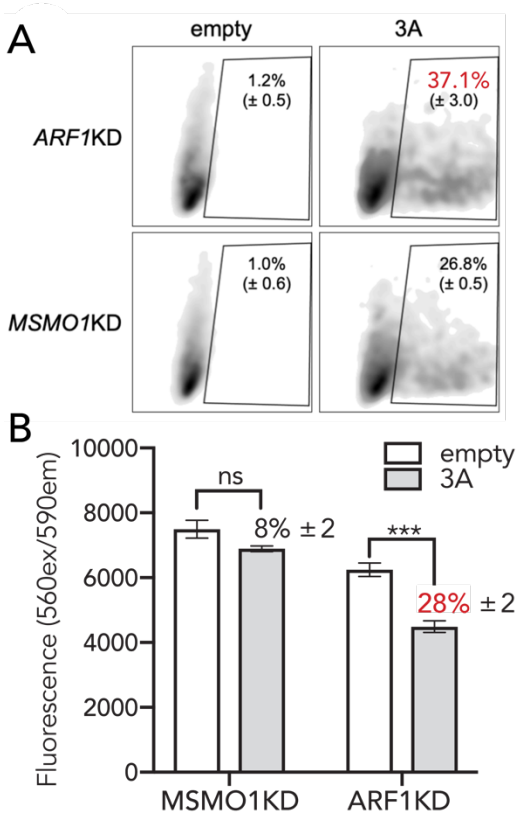

Figure 4: Synthetic lethal killing of a vi-hypomorph of GBF1. A. *ARF1* and a non-SL gene *MSMO1* were stably silenced in HeLa cells and transfected with poliovirus 3A. The expression levels of 3A-FLAG 48 h post transfection were measured by flow cytometry. **B.** Cell viabilities of *ARF1*KD and *MSMO1*KD transfected with 3A-FLAG or empty plasmid control were measured using CellTiterBlue.

Supplemental Figure S1

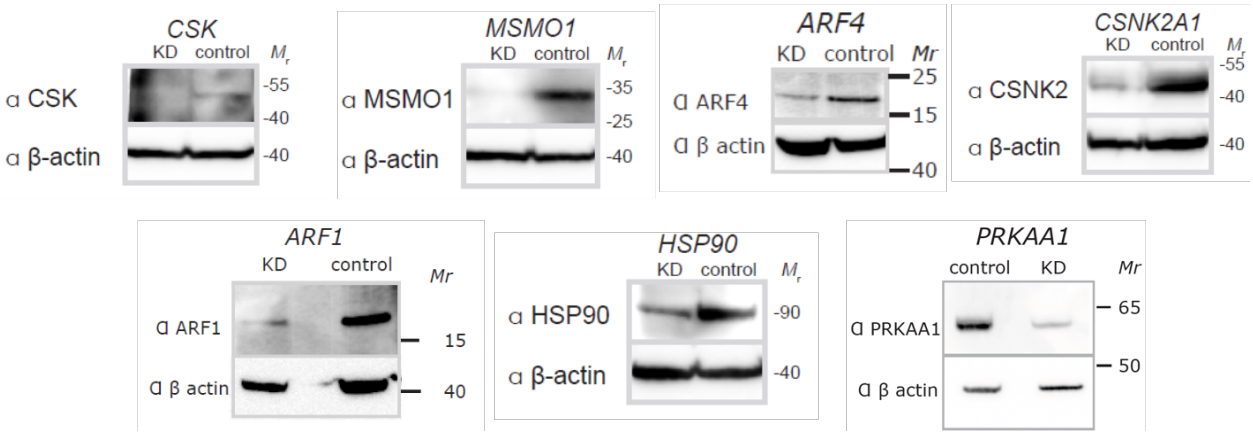

Five druggable putative synthetic lethal partners of GBF1, a a random nonGBF1-SL gene *MSMO1* and the topmost overrepresented gene, *ARF4*, were silenced in Hela cells via shRNA-mediated lentivirus transductions and selected on puromycin for 72 h. Small aliquots of a cell pellet from each KD cell lines were collected, lysed, and total protein concentrations were measured using a standard BCA assay. Equal amounts of total proteins from the control and KD cells were resolved by SDS-PAGE, transferred to nitrocellulose and the presence of each protein of interest was then probed using appropriate antibodies. For the loading control, membranes were stripped, re-blocked and probed using antibodies to β-actin.

REFERENCES

1. Woolhouse M, Gaunt E. Ecological Origins of Novel Human Pathogens. Crit Rev Microbiol [Internet]. 2007 Jan 11;33(4):231–242. Available from: http://www.tandfonline.com/doi/full/10.1080/10408410701647560
2. Sanjuán R, Nebot MR, Chirico N, Mansky LM, Belshaw R. Viral Mutation Rates. J Virol [Internet] PMID: 20660197. American Society for Microbiology; 2010 Oct 1 [cited 2020 Oct 12];84(19):9733–9748. Available from: https://pubmed.ncbi.nlm.nih.gov/20660197/
3. Heaton SM. Harnessing host–virus evolution in antiviral therapy and immunotherapy. Clin Transl Immunol [Internet]. 2019 Jan 8 [cited 2020 Apr 1];8(7). Available from: https://www.ncbi.nlm.nih.gov/pmc/articles/PMC6613463/
4. Woolhouse MEJ, Brierley L. Epidemiological characteristics of human-infective RNA viruses. Sci Data [Internet] PMID: 29461515. Nature Publishing Groups; 2018 Feb 20 [cited 2020 Oct 8];5(1):1–6. Available from: www.nature.com/sdata/
5. Pennings PS. HIV drug resistance: Problems and perspectives. Infect Dis Rep. 2013;5(SUPPL.1):21–25.
6. van der Vries E, Schutten M, Fraaij P, Boucher C, Osterhaus A. Influenza virus resistance to antiviral therapy. Adv Pharmacol. Academic Press Inc.; 2013. p. 217–246.
7. Irwin KK, Renzette N, Kowalik TF, Jensen JD. Antiviral drug resistance as an adaptive process. Virus Evol. Oxford University Press (OUP); 2016 Jan;2(1):vew014.
8. Mast FD, Navare AT, van der Sloot AM, Coulombe-Huntington J, Rout MP, Baliga NS, Kaushansky A, Chait BT, Aderem A, Rice CM, Sali A, Tyers M, Aitchison JD. Crippling life support for SARS-CoV-2 and other viruses through synthetic lethality. J Cell Biol [Internet] PMID: 32785687. NLM (Medline); 2020 Oct 5 [cited 2020 Oct 8];219(10). Available from: https://pubmed.ncbi.nlm.nih.gov/32785687/
9. Brass AL, Dykxhoorn DM, Benita Y, Yan N, Engelman A, Xavier RJ, Lieberman J, Elledge SJ. Identification of host proteins required for HIV infection through a functional genomic screen. Science (80-) [Internet] PMID: 18187620. Science; 2008 Feb 15 [cited 2020 Oct 8];319(5865):921–926. Available from: https://pubmed.ncbi.nlm.nih.gov/18187620/
10. Zhou H, Xu M, Huang Q, Gates AT, Zhang XD, Castle JC, Stec E, Ferrer M, Strulovici B, Hazuda DJ, Espeseth AS. Genome-Scale RNAi Screen for Host Factors Required for HIV Replication. Cell Host Microbe [Internet] PMID: 18976975. Cell Host Microbe; 2008 Nov 13 [cited 2020 Oct 8];4(5):495–504. Available from: https://pubmed.ncbi.nlm.nih.gov/18976975/
11. Krishnan MN, Garcia-Blanco MA. Targeting host factors to treat West Nile and dengue viral infections. Viruses. 2014. p. 683–708.
12. Basler CF, Krogan NJ, Leung DW, Amarasinghe GK. Virus and host interactions critical for filoviral RNA synthesis as therapeutic targets [Internet]. Antiviral Research. Elsevier B.V.; 2019 [cited 2020 Oct 8]. p. 90–100. Available from: https://pubmed.ncbi.nlm.nih.gov/30550800/
13. Saeed M, Kapell S, Hertz NT, Wu X, Bell K, Ashbrook AW, Mark MT, Zebroski HA, Neal ML, Flodström-Tullberg M, MacDonald MR, Aitchison JD, Molina H, Rice CM. Defining the proteolytic landscape during enterovirus infection. Semler BL, editor. PLOS Pathog [Internet]. PLoS Pathog; 2020 Sep 30 [cited 2020 Oct 8];16(9):e1008927. Available from: https://dx.plos.org/10.1371/journal.ppat.1008927
14. Lum KK, Cristea IM. Proteomic approaches to uncovering virus-host protein interactions during the progression of viral infection [Internet]. Expert Review of Proteomics. Taylor and Francis Ltd; 2016 [cited 2020 Oct 8]. p. 325–340. Available from: https://pubmed.ncbi.nlm.nih.gov/26817613/
15. Carpp LN, Rogers RS, Moritz RL, Aitchison JD. Quantitative proteomic analysis of host-

virus interactions reveals a role for golgi brefeldin a resistance factor 1 (GBF1) in dengue infection. Mol Cell Proteomics. American Society for Biochemistry and Molecular Biology Inc.; 2014 Nov 1;13(11):2836–2854.

16. Gordon DE, Jang GM, Bouhaddou M, Xu J, Obernier K, White KM, O'Meara MJ, Rezelj V V., Guo JZ, Swaney DL, Tummino TA, Hüttenhain R, Kaake RM, Richards AL, Tutuncuoglu B, Foussard H, Batra J, Haas K, Modak M, Kim M, Haas P, Polacco BJ, Braberg H, Fabius JM, Eckhardt M, Soucheray M, Bennett MJ, Cakir M, McGregor MJ, Li Q, Meyer B, Roesch F, Vallet T, Mac Kain A, Miorin L, Moreno E, Naing ZZC, Zhou Y, Peng S, Shi Y, Zhang Z, Shen W, Kirby IT, Melnyk JE, Chorba JS, Lou K, Dai SA, Barrio-Hernandez I, Memon D, Hernandez-Armenta C, Lyu J, Mathy CJP, Perica T, Pilla KB, Ganesan SJ, Saltzberg DJ, Rakesh R, Liu X, Rosenthal SB, Calviello L, Venkataramanan S, Liboy-Lugo J, Lin Y, Huang XP, Liu YF, Wankowicz SA, Bohn M, Safari M, Ugur FS, Koh C, Savar NS, Tran QD, Shengjuler D, Fletcher SJ, O'Neal MC, Cai Y, Chang JCJ, Broadhurst DJ, Klippsten S, Sharp PP, Wenzell NA, Kuzuoglu-Ozturk D, Wang HY, Trenker R, Young JM, Cavero DA, Hiatt J, Roth TL, Rathore U, Subramanian A, Noack J, Hubert M, Stroud RM, Frankel AD, Rosenberg OS, Verba KA, Agard DA, Ott M, Emerman M, Jura N, von Zastrow M, Verdin E, Ashworth A, Schwartz O, d'Enfert C, Mukherjee S, Jacobson M, Malik HS, Fujimori DG, Ideker T, Craik CS, Floor SN, Fraser JS, Gross JD, Sali A, Roth BL, Ruggero D, Taunton J, Kortemme T, Beltrao P, Vignuzzi M, García-Sastre A, Shokat KM, Shoichet BK, Krogan NJ. A SARS-CoV-2 protein interaction map reveals targets for drug repurposing. Nature [Internet] PMID: 32353859. Nature Research; 2020 Jul 16 [cited 2020 Oct 8];583(7816):459–468. Available from: https://pubmed.ncbi.nlm.nih.gov/32353859/
17. Stukalov A, Girault V, Grass V, Bergant V, Karayel O, Urban C, Haas DA, Huang Y, Oubraham L, Wang A, Hamad SM, Piras A, Tanzer M, Hansen FM, Enghleitner T, Reinecke M, Lavacca TM, Ehmann R, Wölfel R, Jores J, Kuster B, Protzer U, Rad R, Ziebuhr J, Thiel V, Scaturro P, Mann M, Pichlmair A. Multi-level proteomics reveals host-perturbation strategies of SARS-CoV-2 and SARS-CoV. bioRxiv [Internet]. Cold Spring Harbor Laboratory; 2020 Jun 17 [cited 2020 Oct 8];2020.06.17.156455. Available from: https://doi.org/10.1101/2020.06.17.156455
18. Meyniel-Schicklin L, De Chassey B, André P, Lotteau V. Viruses and interactomes in translation. Mol Cell Proteomics. 2012;
19. de Chassey B, Meyniel-Schicklin L, Vonderscher J, André P, Lotteau V. Virus-host interactomics: New insights and opportunities for antiviral drug discovery. Genome Medicine. BioMed Central Ltd.; 2014.
20. Pfefferle S, Schöpf J, Kögl M, Friedel CC, Müller MA, Carbajo-Lozoya J, Stellberger T, von Dall'Armi E, Herzog P, Kallies S, Niemeyer D, Ditt V, Kuri T, Züst R, Pumpor K, Hilgenfeld R, Schwarz F, Zimmer R, Steffen I, Weber F, Thiel V, Herrler G, Thiel H-J, Schwegmann-Weßels C, Pöhlmann S, Haas J, Drosten C, von Brunn A. The SARS-Coronavirus-Host Interactome: Identification of Cyclophilins as Target for Pan-Coronavirus Inhibitors. Denison MR, editor. PLoS Pathog [Internet]. 2011 Oct 27 [cited 2019 Dec 24];7(10):e1002331. Available from: http://dx.plos.org/10.1371/journal.ppat.1002331
21. Navratil V, De chassey B, Meyniel L, Delmotte S, Gautier C, André P, Lotteau V, Rabourdin-Combe C. VirHostNet: A knowledge base for the management and the analysis of proteome-wide virus-host interaction networks. Nucleic Acids Res. 2009;
22. DOBZHANSKY T. Genetics of natural populations; recombination and variability in populations of Drosophila pseudoobscura. Genetics. 1946;
23. Nijman SMB. Synthetic lethality: General principles, utility and detection using genetic screens in human cells [Internet]. FEBS Letters. Elsevier B.V.; 2011 [cited 2020 Sep 24]. p. 1–6. Available from: https://pubmed.ncbi.nlm.nih.gov/21094158/

24. Boone C, Bussey H, Andrews BJ. Exploring genetic interactions and networks with yeast. Nature Reviews Genetics. 2007.
25. Dixon SJ, Andrews BJ, Boone C. Exploring the conservation of synthetic lethal genetic interaction networks. Commun Integr Biol. 2009;
26. Horlbeck MA, Xu A, Wang M, Bennett NK, Park CY, Bogdanoff D, Adamson B, Chow ED, Kampmann M, Peterson TR, Nakamura K, Fischbach MA, Weissman JS, Gilbert LA. Mapping the Genetic Landscape of Human Cells. Cell. 2018;
27. McManus KJ, Barrett IJ, Nouhi Y, Hieter P. Specific synthetic lethal killing of RAD54B-deficient human colorectal cancer cells by FEN1 silencing. Proc Natl Acad Sci U S A. 2009;
28. Kaelin WG. The concept of synthetic lethality in the context of anticancer therapy. Nature Reviews Cancer. 2005.
29. Turner NC, Lord CJ, Iorns E, Brough R, Swift S, Elliott R, Rayter S, Tutt AN, Ashworth A. A synthetic lethal siRNA screen identifying genes mediating sensitivity to a PARP inhibitor. EMBO J. 2008;
30. Farmer H, McCabe H, Lord CJ, Tutt AHJ, Johnson DA, Richardson TB, Santarosa M, Dillon KJ, Hickson I, Knights C, Martin NMB, Jackson SP, Smith GCM, Ashworth A. Targeting the DNA repair defect in BRCA mutant cells as a therapeutic strategy. Nature. 2005 Apr 14;434(7035):917–921.
31. Wiltshire TD, Lovejoy CA, Wang T, Xia F, O'Connor MJ, Cortez D. Sensitivity to poly(ADP-ribose) polymerase (PARP) inhibition identifies ubiquitin-specific peptidase 11 (USP11) as a regulator of DNA double-strand break repair. J Biol Chem. 2010;
32. Mendes-Pereira AM, Martin SA, Brough R, McCarthy A, Taylor JR, Kim JS, Waldman T, Lord CJ, Ashworth A. Synthetic lethal targeting of PTEN mutant cells with PARP inhibitors. EMBO Mol Med. 2009;
33. Bryant HE, Schultz N, Thomas HD, Parker KM, Flower D, Lopez E, Kyle S, Meuth M, Curtin NJ, Helleday T. Specific killing of BRCA2-deficient tumours with inhibitors of poly(ADP-ribose) polymerase. Nature. 2005;
34. Litton JK, Rugo HS, Ettl J, Hurvitz SA, Gonçalves A, Lee KH, Fehrenbacher L, Yerushalmi R, Mina LA, Martin M, Roché H, Im YH, Quek RGW, Markova D, Tudor IC, Hannah AL, Eiermann W, Blum JL. Talazoparib in patients with advanced breast cancer and a germline BRCA mutation. N Engl J Med. 2018;
35. Thaker SK, Ch'ng J, Christofk HR. Viral hijacking of cellular metabolism. BMC biology. NLM (Medline); 2019. p. 59.
36. Gaur P, Munjal A, Lal SK. Influenza virus and cell signaling pathways. Medical Science Monitor. International Scientific Literature Inc.; 2011.
37. Belov GA, Altan-Bonnet N, Kovtunovych G, Jackson CL, Lippincott-Schwartz J, Ehrenfeld E. Hijacking Components of the Cellular Secretory Pathway for Replication of Poliovirus RNA. J Virol. American Society for Microbiology; 2007 Jan 15;81(2):558–567.
38. Claude A, Zhao B-P, Kuziemsky CE, Dahan S, Berger SJ, Yan J-P, Armold AD, Sullivan EM, Melançon P. GBF1: A Novel Golgi-associated BFA-resistant Guanine Nucleotide Exchange Factor That Displays Specificity for ADP-ribosylation Factor 5 [Internet]. The Journal of Cell Biology. 1999. Available from: http://www.jcb.org
39. Donaldson JG, Jackson CL. ARF family G proteins and their regulators: Roles in membrane transport, development and disease. Nature Reviews Molecular Cell Biology. 2011. p. 362–375.
40. Sáenz JB, Sun WJ, Chang JW, Li J, Bursulaya B, Gray NS, Haslam DB. Golgicide A reveals essential roles for GBF1 in Golgi assembly and function. Nat Chem Biol. Nature Publishing Group; 2009;5(3):157–165.
41. Beller M, Sztalryd C, Southall N, Bell M, Jäckle H, Auld DS, Oliver B. COPI complex is a regulator of lipid homeostasis. PLoS Biol. Public Library of Science; 2008;6(11):2530–

2549.
42. Guo Y, Walther TC, Rao M, Stuurman N, Goshima G, Terayama K, Wong JS, Vale RD, Walter P, Farese R V. Functional genomic screen reveals genes involved in lipid-droplet formation and utilization. Nature. Nature Publishing Group; 2008 May 29;453(7195):657–661.
43. Soni KG, Mardones GA, Sougrat R, Smirnova E, Jackson CL, Bonifacino JS. Coatomer-dependent protein delivery to lipid droplets. J Cell Sci. 2009 Jun 1;122(11):1834–1841.
44. Kaczmarek B, Verbavatz JM, Jackson CL. GBF1 and Arf1 function in vesicular trafficking, lipid homoeostasis and organelle dynamics. Biology of the Cell. 2017.
45. Belov GA, Feng Q, Nikovics K, Jackson CL, Ehrenfeld E. A critical role of a cellular membrane traffic protein in poliovirus RNA replication. PLoS Pathog. 2008 Nov;4(11).
46. Lanke KHW, van der Schaar HM, Belov GA, Feng Q, Duijsings D, Jackson CL, Ehrenfeld E, van Kuppeveld FJM. GBF1, a Guanine Nucleotide Exchange Factor for Arf, Is Crucial for Coxsackievirus B3 RNA Replication. J Virol. American Society for Microbiology; 2009 Nov 15;83(22):11940–11949.
47. Verheije MH, Raaben M, Mari M, Te Lintelo EG, Reggiori F, Van Kuppeveld FJM, Rottier PJM, De Haan CAM. Mouse hepatitis coronavirus RNA replication depends on GBF1-mediated ARF1 activation. PLoS Pathog. 2008 Jun;4(6).
48. Goueslain L, Alsaleh K, Horellou P, Roingeard P, Descamps V, Duverlie G, Ciczora Y, Wychowski C, Dubuisson J, Rouille Y. Identification of GBF1 as a Cellular Factor Required for Hepatitis C Virus RNA Replication. J Virol. American Society for Microbiology; 2010 Jan 15;84(2):773–787.
49. Farhat R, Ankavay M, Lebsir N, Gouttenoire J, Jackson CL, Wychowski C, Moradpour D, Dubuisson J, Rouillé Y, Cocquerel L. Identification of GBF1 as a cellular factor required for hepatitis E virus RNA replication. Cell Microbiol. Blackwell Publishing Ltd; 2018 Jan 1;20(1).
50. Yamayoshi S, Neumann G, Kawaoka Y. Role of the GTPase Rab1b in Ebolavirus Particle Formation. J Virol. American Society for Microbiology; 2010 May 1;84(9):4816–4820.
51. Martínez J, Arnoldi F, Schraner E, Eichwald C, Silva-Ayala D, Lee E, Sztul E, Burrone Ó, López S, Arias C. The guanine nucleotide exchange factor GBF1 participates in rotavirus replication. bioRxiv. 2019;619924.
52. Belov GA, Feng Q, Nikovics K, Jackson CL, Ehrenfeld E. A critical role of a cellular membrane traffic protein in poliovirus RNA replication. PLoS Pathog. 2008;
53. Teterina NL, Pinto Y, Weaver JD, Jensen KS, Ehrenfeld E. Analysis of Poliovirus Protein 3A Interactions with Viral and Cellular Proteins in Infected Cells. J Virol. 2011;
54. Wessels E, Duijsings D, Lanke KHW, van Dooren SHJ, Jackson CL, Melchers WJG, van Kuppeveld FJM. Effects of Picornavirus 3A Proteins on Protein Transport and GBF1-Dependent COP-I Recruitment. J Virol. American Society for Microbiology; 2006 Dec 1;80(23):11852–11860.
55. Wessels E, Duijsings D, Niu TK, Neumann S, Oorschot VM, de Lange F, Lanke KHW, Klumperman J, Henke A, Jackson CL, Melchers WJG, van Kuppeveld FJM. A Viral Protein that Blocks Arf1-Mediated COP-I Assembly by Inhibiting the Guanine Nucleotide Exchange Factor GBF1. Dev Cell [Internet] PMID: 16890159. Dev Cell; 2006 Aug [cited 2020 Sep 30];11(2):191–201. Available from: https://pubmed.ncbi.nlm.nih.gov/16890159/
56. Wessels E, Duijsings D, Lanke KHW, van Dooren SHJ, Jackson CL, Melchers WJG, van Kuppeveld FJM. Effects of Picornavirus 3A Proteins on Protein Transport and GBF1-Dependent COP-I Recruitment. J Virol [Internet] PMID: 17005635. American Society for Microbiology; 2006 Dec 1 [cited 2020 Oct 8];80(23):11852–11860. Available from: https://pubmed.ncbi.nlm.nih.gov/17005635/
57. Wessels E, Duijsings D, Lanke KHW, Melchers WJG, Jackson CL, van Kuppeveld FJM. Molecular Determinants of the Interaction between Coxsackievirus Protein 3A and

Guanine Nucleotide Exchange Factor GBF1. J Virol. American Society for Microbiology; 2007 May 15;81(10):5238–5245.
58. Richards AL, Soares-Martins JAP, Riddell GT, Jackson WT. Generation of unique poliovirus RNA replication organelles. MBio. American Society for Microbiology; 2014 Feb 25;5(2).
59. Bertomeu T, Coulombe-Huntington J, Chatr-aryamontri A, Bourdages KG, Coyaud E, Raught B, Xia Y, Tyers M. A High-Resolution Genome-Wide CRISPR/Cas9 Viability Screen Reveals Structural Features and Contextual Diversity of the Human Cell-Essential Proteome. Mol Cell Biol [Internet]. American Society for Microbiology; 2018 Jan 1 [cited 2020 Oct 9];38(1). Available from: /pmc/articles/PMC5730719/?report=abstract
60. Wang T, Wei JJ, Sabatini DM, Lander ES. Genetic screens in human cells using the CRISPR-Cas9 system. Science (80-). 2014;
61. Spang A. ARF1 regulatory factors and COPI vesicle formation. Current Opinion in Cell Biology. 2002.
62. Rowlands M, McAndrew C, Prodromou C, Pearl L, Kalusa A, Jones K, Workman P, Aherne W. Detection of the ATPase activity of the molecular chaperones Hsp90 and Hsp72 using the transcreener™ ADP assay kit. J Biomol Screen [Internet] PMID: 20147598. J Biomol Screen; 2010 [cited 2020 Oct 12];15(3):279–286. Available from: https://pubmed.ncbi.nlm.nih.gov/20147598/
63. Okada M. Regulation of the Src family kinases by Csk [Internet]. International Journal of Biological Sciences. Ivyspring International Publisher; 2012 [cited 2020 Oct 12]. p. 1385–1397. Available from: /pmc/articles/PMC3492796/?report=abstract
64. Sanli T, Steinberg GR, Singh G, Tsakiridis T. AMP-activated protein kinase (AMPK) beyond metabolism: A novel genomic stress sensor participating in the DNA damage response pathway [Internet]. Cancer Biology and Therapy. Landes Bioscience; 2014 [cited 2020 Oct 12]. p. 156–169. Available from: https://www.tandfonline.com/doi/abs/10.4161/cbt.26726
65. Allada R, Meissner RA. Casein kinase 2, circadian clocks, and the flight from mutagenic light [Internet]. Molecular and Cellular Biochemistry. Mol Cell Biochem; 2005 [cited 2020 Oct 12]. p. 141–149. Available from: https://pubmed.ncbi.nlm.nih.gov/16335534/
66. Yamane K, Kinsella TJ. Casein kinase 2 regulates both apoptosis and the cell cycle following DNA damage induced by 6-thioguanine. Clin Cancer Res [Internet] PMID: 15788687. American Association for Cancer Research; 2005 Mar 15 [cited 2020 Oct 12];11(6):2355–2363. Available from: https://clincancerres.aacrjournals.org/content/11/6/2355
67. Nijman SMB. Synthetic lethality: General principles, utility and detection using genetic screens in human cells. FEBS Letters. Elsevier B.V.; 2011. p. 1–6.
68. Mast FD, Herricks T, Strehler KM, Miller LR, Saleem RA, Rachubinski RA, Aitchison JD. ESC RT-III is required for scissioning new peroxisomes from the endoplasmic reticulum. J Cell Biol [Internet] PMID: 29588378. Rockefeller University Press; 2018 Jun 1 [cited 2020 Oct 8];217(6):2087–2102. Available from: https://pubmed.ncbi.nlm.nih.gov/29588378/
69. Vijayan K, Cestari I, Mast FD, Glennon EKK, McDermott SM, Kain HS, Brokaw AM, Aitchison JD, Stuart K, Kaushansky A. Plasmodium Secretion Induces Hepatocyte Lysosome Exocytosis and Promotes Parasite Entry. iScience [Internet]. Elsevier Inc.; 2019 Nov 22 [cited 2020 Oct 8];21:603–611. Available from: https://pubmed.ncbi.nlm.nih.gov/31731198/
70. Cristea IM, Chait BT. Conjugation of magnetic beads for immunopurification of protein complexes. Cold Spring Harb Protoc. 2011;